Stability of diamond at high pressures

A. F. Goncharov

A. V. Shubnikov Institute of Crystallography, Academy of Sciences of the USSR, Moscow

Usp. Fiz. Nauk **152**, 317–332 (June 1987)

CONTENTS

1. INTRODUCTION

Diamond is a typical representative of the class of tetrahedral covalent crystals. The crystal structure of diamond represents an open network of coordination tetrahedra (Fig. 1a) which fills only part of the available space.[1)] This is the reason for the instability of diamond (α-phase) structures at high pressures compared with structures with the closer packing, a property shared with all the investigated structure analogs of diamond. In particular, the closest analogs of diamond—silicon (Si) and germanium (Ge)—exhibit a transition to the structure of white tin (β-Sn or simply β) at relatively low pressures (~ 100 kbar).[2)] The $\alpha \rightarrow \beta$ transition modifies the tetrahedral coordination of the atoms due to the sp^3 hybridization of the valence orbitals, and gives rise to a new dense metallic phase with a sixfold coordination (Fig. 1b). It is interesting to note that in spite of some increase (by 9%) in the interatomic space between the nearest neighbors in the metallic β phase, this phase is 20% denser than the α phase because of an increase in the coordination number.

In the case of atomic carbon the situation is largely uncertain because of the absence of reliable experimental data at high pressures and temperatures. Therefore, the phase diagram of carbon has for a long time been based on various scaling relationships.

A new understanding of the phase diagram of carbon at ultrahigh pressures began to develop from the time of appearance of the theoretical paper of Yin and Cohen[1] who postulated that the diamond phase is the densest among all possible metal structures up to ~ 23 Mbar. If this is indeed true, then diamond is not a typical but an exceptional member of the family of tetrahedral covalent crystals differing from its analogs by a unique stability of the crystal lattice.

We shall now review the available experimental and theoretical data on the problem of stability of the diamond structure of carbon. For comparison, we shall consider also the data on its closest analogs (mainly Si and Ge).

2. PHASE DIAGRAMS OF CARBON AND ITS CLOSEST ANALOGS Si, Ge, Sn

The phase diagrams of Si, Ge, and Sn have been investigated in considerable detail in the range of stability of the α phase and in the immediate vicinity of this range[2–26] (Fig. 2). We can see from Fig. 2 that the P-T diagrams of Si, Ge, and Sn are generally similar and are characterized by the existence of three phases: α and β described above, and a metallic liquid (l). The melting curve[3)] of the α phase always has a negative slope and, consequently, the liquid is a denser phase than the "open" structure of the α phase. At high pressures both Si and Ge undergo a transition to the metallic solid β phase. A similar transition occurs in Sn at atmospheric pressure and $T = 286$ K. The α-l and α-β phase equilibrium curves intersect at the triple point representing a phase equilibrium between the α, β, and l phases and also the origin of the melting curve of the β phase which has a positive slope.

In addition to the α, β, and l phases mentioned above, the elements Si and Ge have several other modifications which clearly have no stability regions in the equilibrium P-T diagram, but exist under atmospheric conditions. Lowering of the pressure transforms the β phases of Si and Ge to Si

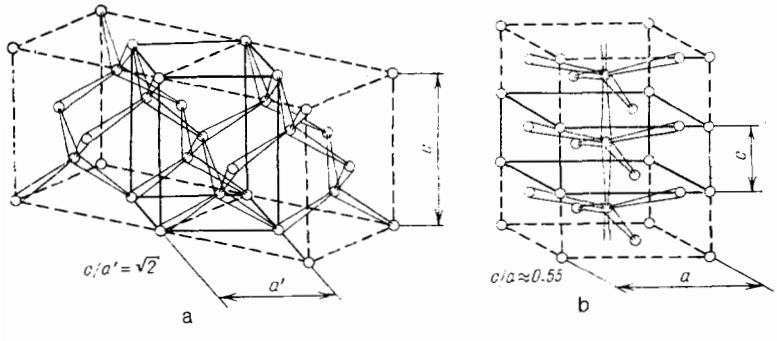

FIG. 1. Comparison of the unit cells of diamond (a) and white tin (b). The tetragonal cell, which is the prototype of the unit cell of white tin, is identified by continuous lines in Fig. 1a.

 0038-5670/87/060525-10$01.80

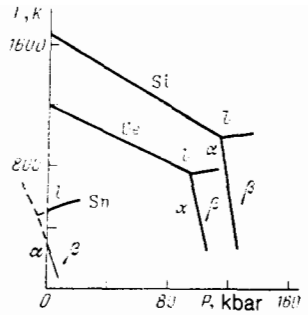

FIG. 2. Phase diagrams of Si, Ge, and Sn. Here α, β, and l are the regions of stability of the diamond phase, the white tin phase, and a metallic liquid, respectively.

III and Ge III (Fig. 3), the structures of which have been determined and found to be bcc with $Z = 16$ (BC-8) and tetragonal with $Z = 12$ (ST-12), respectively.[11,24,25] The phases with the BC-8 and ST-12 structures have a slightly distorted tetrahedral coordination of the atoms and are approximately 10% denser than the corresponding α phases. Application of pressures of 110–130 kbar to samples cooled with dry ice produces a Ge IV phase,[26] which is a structural analog of Si III. At room temperature the Ge IV phase gradually transforms to Ge III. The Si III and Ge III phases are stable up to temperatures ~120–150 °C and at 200–600 °C are transformed to the hexagonal ($h\alpha$) and cubic (α) diamond phases, respectively.[11,24] The hexagonal diamond phase $h\alpha$ has the same density and the same coordination of the nearest neighbors as the cubic diamond modification, but differs from the latter in respect of the coordination of the second-nearest neighbors.

Recent investigations have revealed an additional allo-Ge phase with an orthorhombic lattice, formed as a result of chemical processes.[27] This has led to the proposal[28] of a whole class of quasitwo-dimensional structures for group IV crystal compounds. In the case of Si the density of such a structure is 1.3% less than the density of the diamond phase.

The available data on the phase diagram of carbon are discussed in detail in reviews.[29,30] Therefore, we shall describe briefly the main results and concentrate our attention on possible transformations of diamond to a denser modification.

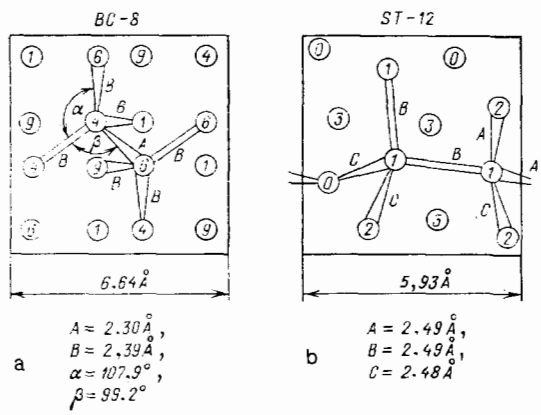

FIG. 3. Projections of the unit cells of the Si III (a) and Ge III (b) structures onto the (x,y) plane.[25] The number inside the circle representing an atom gives its coordinate in fractions of the lattice constant multiplied by 10 in Fig. 3a and by 4 in Fig. 3b.

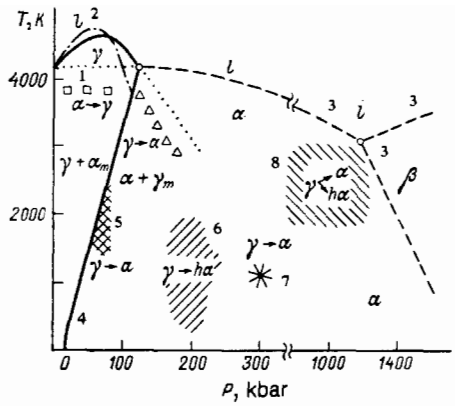

FIG. 4. Phase diagram of atomic carbon.[29,39] Notation: α, γ, β, and l are the regions of stability of the diamond, graphite, metallic, and liquid phases, respectively; α_m and γ_m are the metastable diamond and graphite phases; 1) postulated melting curves of the phases γ_m and α_m, respectively (explanations in text); 2) melting curve of graphite according to Ref. 38; 3) postulated boundaries between phases α, β, and l; 4) boundaries between the phases α, γ, and l according to Ref. 39; 5) region of industrial catalytic synthesis of diamond; 6) region of formation of hexagonal diamond from graphite in static experiments[40,41]; 7) formation of the diamond phase in dynamic experiments[41]; 8) range of formation of diamond phases in dynamic experiments.[50] Note the discontinuity and the change in scale along the P axis.

Figure 4 gives one of the latest versions of the phase diagram of carbon proposed by Bundy[29] on the basis of various analogies and supported by few experimental data. The most striking difference between the phase diagram of carbon and the corresponding diagrams of Si and Ge is the existence of the graphite phase (γ) representing a quasitwo-dimensional crystalline modification of carbon.[4)] The equilibrium line between the α and γ phases has been determined very accurately both experimentally[32,33] and also by means of thermodynamic calculations.[34-36] The region of industrial catalytic synthesis of diamond from graphite (shown shaded in Fig. 4) is located near this line. The melting curve of graphite was investigated experimentally by a variety of methods both by Bundy[37] and by Fateeva and Vereshchagin.[38] This curve has a maximum at a pressure of ~70 kbar and it terminates at the triple point of a phase equilibrium between the α, γ, and l phases.[32,33,36-39] Melting of the diamond phase of carbon at pressures slightly higher than the triple point seems to have been observed by Bundy,[39b] but the results were qualitative and insufficient to determine even the sign of the initial slope of the melting curve of diamond. The data on direct transitions from graphite to diamond (triangles in Fig. 4) and from diamond to graphite (squares in Fig. 4) obtained by Bundy[39] are of special interest. The lines representing these results have been interpreted as the boundaries of the absolute instability of the γ and α phases, respectively. According to Bundy,[39] the mechanism of these fast $\gamma \rightarrow \alpha$ and $\alpha \rightarrow \gamma$ transformations includes pseudomelting of the metastable phase and then crystallization producing a phase which is stable at a given point in the P-T diagram. Therefore, data on pseudomelting of the α phase (graphitization of diamond) give some idea on the nature of the melting curve of the diamond phase at pressures above the triple point. We can tentatively draw from them the conclusion that the initial slope of the melting curve of diamond is practically zero.

At pressures of ~200 kbar and temperatures from

room to 2000 °C (Fig. 4) the metastable (in this part of the P-T diagram) graphite phase is transformed into a new form of carbon.[40,41] Heating to 1000 °C or higher temperatures makes it possible to retain this phase after the removal of pressure. An x-ray structure investigation demonstrated[41] that the new phase of carbon represents hexagonal diamond (lonsdaleite). This phase is most likely, like the corresponding phases of Si (Ref. 24) and BN (Ref. 42), a metastable modification without its place in the equilibrium P-T diagram.

The diamond phases α and hα of carbon can also form under dynamic conditions and, moreover, they have been found in meteorites.[43] An examination of the extensive literature on the dynamic experiments on graphite[44–52] shows that the results depend very strongly on the experimental conditions, such as the initial density and temperature of a sample, its structure and orientation, the material from which a striker is made, the parameters of quenching after unloading, etc. Therefore, many of the results obtained cannot be interpreted unambiguously and this has given rise to proposals of various speculative variants of the phase diagram of carbon at ultrahigh pressures and temperatures. Initially, the phase diagram of carbon at pressures exceeding 100 kbar was plotted using the results of dynamic experiments of Alder and Christian[44] who reported the discovery of a new, 15% denser than diamond, carbon phase at pressures above 500 kbar, identified tentatively as a metallic liquid. Since a disturbance of the tetrahedral coordination of atoms in the closest structural analogs of diamond results in a very similar volume discontinuity, some authors[2,3,39] have proposed a phase diagram of diamond similar to the well-known phase diagrams of Si, Ge, InSb, and other III–V compounds with the zinc-blende structure. Consequently, Bundy[39] interpreted the results of the dynamic experiments on graphite samples with different initial densities[44] as melting of the α phase of carbon and proposed the existence above 600 kbar of a solid metallic "phase III" representing an analog of the high-pressure phases of Ge and InSb crystals.[5)] It is not quite clear to the author of the present review how the pressure causing the $I(\alpha) \rightarrow III$ transformation was estimated. However, an analogous critical transition pressure ($\sim$650 kbar) is obtained if it is assumed that the reduced pressure of the transition P_c/K, where K is the bulk modulus, is constant for all the crystals undergoing the $\alpha \rightarrow \beta$ transition at high pressures. The triple point of the equilibrium between the phases α, l, and "phase III" in the first phase diagram of carbon proposed by Bundy is located at $P \approx 650$ kbar and $T \approx 1200$ K. Jayaraman *et al.*[2] suggested the use of the triple point at $P \approx 600$ kbar and $T \approx 2700$ K, because the slope of the melting curve of the α phase in the Bundy variant is too high (-6 K/kbar) and does not agree with the corresponding slopes of other substances. The volume discontinuity found in the experiments of Alder and Christian[44] is then interpreted as the $\alpha \rightarrow \beta$ transition.

Soon after many more dynamic experiments were carried out on graphite[46–48,52] and these demonstrated the errors of the results in the much-quoted paper of Alder and Christian on the appearance of a metallic state of carbon. In view of this, it is necessary to postulate that the transformation of diamond to a denser metallic phase should occur at higher pressures.

Jamieson[53] obtained an empirical relationship $P_c \Delta V = \Delta E/2$ between the parameters of the transitions in IV and III–V semiconductors to a metallic state and the width of the band gap of these materials. Jamieson was the first to point out that carbon does not fit the general relationship and explained this qualitatively by the absence of the p electrons in the ionic core. Musgrave[54] derived similar approximate relationships on the assumption that the main driving mechanism of the $\alpha \rightarrow \beta$ transitions is destabilization of the electron configuration in the diamond structure. Estimates of the pressure necessary for the transition of carbon to a metallic state obtained in this way ranged from 1 to 4 Mbar. Similar values were obtained also from a more detailed semiempirical calculation of the energy band structure of the deformed diamond lattice by the atomic orbital (LCAO) method.[55] The work of Weigel *et al.*[55] was stimulated by the observation of a diamond-metal phase transition at static pressures of $\sim$1 Mbar in apparatus with carbonado anvils.[56,57]

Van Vechten[58] used information on the electron structure of tetrahedrally coordinated IV and III–V semiconductors in calculations of phase diagrams which were found to be in excellent agreement with the experimental results on the assumption that solid metallic phases of these compounds have the white tin structure. The results of a calculation of the phase diagram of carbon, which is essentially a more complex variant of the application of the scaling hypothesis using data on the investigated compounds (such as ionicity, melting point at zero pressure, electronic energy band structure, etc.) can be found in Fig. 5a. The $\alpha \rightarrow \beta$ phase transition is predicted to occur at $\sim$1.7 Mbar and the triple point of the equilibrium between the α, β, and l phases should be located in the vicinity of 1.2 Mbar and 3000 K. The position of this point was used by Bundy[29] to construct the second variant of the phase diagram of carbon (Fig. 4).

Grover[59] attempted to calculate the phase diagram of carbon by matching phenomenological models of the equa-

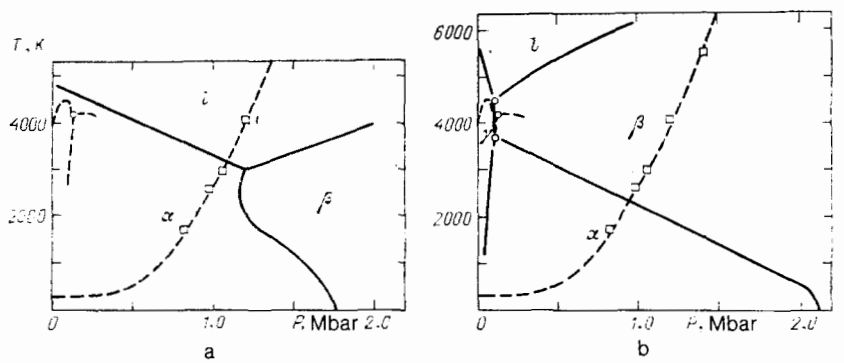

FIG. 5. Calculated phase diagrams of carbon: a) according to Ref. 58; b) according to Ref. 59. The dashed curves near the ordinate represent the experimental results (Fig. 4). The dashed curves and the symbols in the middle of the figure give the results of shock experiments. [52] The designations of the phases are the same as in Fig. 4.

tions of state of various phases of carbon to the available results of ultrasonic and dynamic experiments. The best, in this sense, was found to be a variant of the phase diagram shown in Fig. 5b. According to Grover, diamond does not melt at all at high pressures and temperatures and it is converted directly to the metallic β structure, which in turn melts at still higher temperatures. Grover predicted that the $\alpha \rightarrow \beta$ transition at room temperature should occur at ~ 2 Mbar.

All these investigations of the phase diagram of carbon at high pressures have been essentially based on the hypothesis of the existence of a universal phase diagram for tetrahedral IV and III–V materials (scaling hypothesis). However, the results of the mainly recent dynamic and static experiments carried out at ultrahigh pressures raise doubts about the fruitfulness of this approach. The results of the latest (known to the present author) dynamic experiments on graphite carried out in the range 0.8–1.4 Mbar (Ref. 52) demonstrate that the diamond phase remains solid even in this range of pressures (Fig. 5). Since at the highest pressure the temperature of a sample can reach 5500 K, this means that—in contrast to its analogs—diamond has a melting curve with a positive slope. Shock compression of diamond[60] has failed to reveal any anomalies right up to 5 Mbar, which is considerably higher than all the above-mentioned estimates of the pressure of the $\alpha \rightarrow \beta$ transition. The stability of the diamond structure of carbon at ultrahigh pressures is confirmed also by the whole experience gained in the work using diamond anvils in the megabar range.[61–67] The maximum pressure reached using diamond anvils is ~ 2.75 Mbar (Ref. 62) and this can be regarded as the lower limit of the experimental value of the critical pressure for the diamond-metal transition. Therefore, the tetrahedral configuration of carbon atoms is extremely stable. This fact cannot be explained by the above semiempirical approaches based on the scaling hypothesis.

3. LATTICE DYNAMICS OF TETRAHEDRAL CRYSTALS

The dynamics of a lattice and its stability are closely related. Therefore, the main conclusion of the preceding section can best be checked by a comparative analysis of the vibrational properties of the α phases of C, Si, and Ge, especially as these properties have been investigated very thoroughly. The lattice dynamics of tetrahedral compounds has been for many years the object of continuous attention. The evolution of the views on this topic is described in detail in Refs. 68–74. The majority of the theoretical models have been semiempirical,[68,73] but the potentialities of calculations from first principles has been demonstrated successfully in recent years.[78–80]

The key to the understanding of the characteristics of the dynamics of tetrahedral crystals with the diamond structure is the circumstance that the diamond lattice with exceptionally central short-range interactions is *a priori* unstable because it does not resist shear stresses in the (110) planes, which correspond to transverse acoustic modes near the edge of the Brillouin zone at the points X and L [TA(X) and TA(L)], and also to a long-wavelength acoustic TA1 mode (direction of propagation [110], polarization [$1\bar{1}0$]), related to the elastic modulus $(C_{11} - C_{12})/2$. It should be noted that the macroscopic deformation $(\varepsilon, \varepsilon, -2\varepsilon)$ corresponding to the latter mode does in fact transform the diamond lattice to the lattice of white tin.[81]

Figure 6 shows schematically the displacements of atoms corresponding to the phonon modes at the center of the Brillouin zone (Γ) and at the point X, as well as the deformations associated with the elastic modulus $(C_{11} - C_{12})/2$. It is clear from this figure that the TA1 and TA(X) modes cause basically bending of the bonds and a much weaker stretching, but no compression of the bonds. Consequently, the stability of the diamond lattice against the TA(X) and TA1 modes is ensured by a noncentral interaction which is essentially of covalent nature and is related to the concentration of the valence charges on the bonds.[69,72,74,78]

In the case of transverse and longitudinal optical (TO and LO) and longitudinal acoustic (LA) modes it is found that, in contrast to the TA modes, that the primary effects are compression and stretching of rigid bonds between the nearest neighbors, whereas the bond bending plays a secondary role.[74,77]

It follows from this discussion that the frequencies of the TA modes (compared with the frequencies of the TO, LO, and LA modes) could be used to judge the importance of the noncentral interactions in a crystal and, consequently, the stability of its lattice. The higher the frequencies of the modes (the higher the velocity of sound for the TA1 mode), the greater the resistance of the lattice to shear and the higher the stability.

An important property of the transverse acoustic modes in tetrahedral crystals is the circumstance that they usually have negative Grüneisen parameters (we shall see later that the exceptions to this rule are diamond and boron nitride, the latter known under the trade name of Borazon), $\gamma = -d(\ln\nu)/d(\ln V)$, which is a clear indication of the approaching instability of the lattice against shear deformations in the (110) planes. As shown in Ref. 74, softening of the TA(X) and TA1 modes is a consequence of the fact that the stabilizing noncentral interactions decrease in importance on reduction in the volume (increase in the pressure).

Figure 7 shows the phonon dispersion curves of diamond, Si, and Ge along the [100] and [111] directions obtained by the neutron inelastic scattering method. The dispersion curves of silicon and germanium have the characteristic feature mentioned above and typical of almost all (except for diamond) investigated tetrahedral compounds: there are low-frequency transverse acoustic modes, which become significantly flatter away from the Brillouin

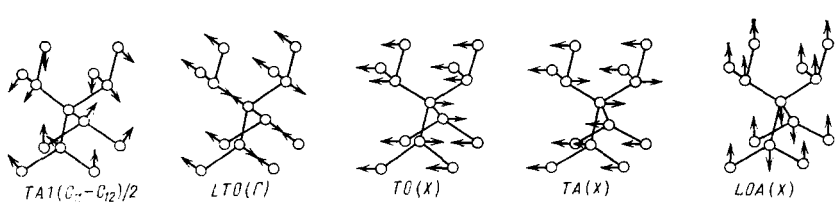

FIG. 6. Displacements of atoms in the case of vibration modes at the points Γ and X in the Brillouin zone. Here, TA1 is a long-wavelength acoustic mode (explanations in text); $\mathrm{LTO}(\Gamma) = \mathrm{LO}(\Gamma) + \mathrm{TO}(\Gamma)$; $\mathrm{LOA}(\mathrm{X}) = \mathrm{LO}(\mathrm{X}) + \mathrm{LA}(\mathrm{X})$.

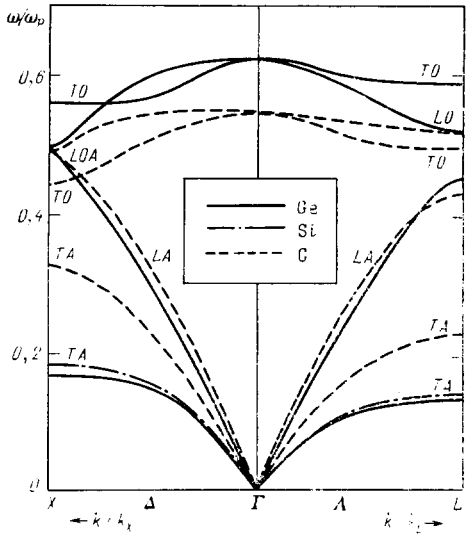

FIG. 7. Phonon dispersion curves of C (diamond), Si, and Ge along the [100] (Δ) and [111] (Λ) directions.[70] The phonon energies are normalized to the plasma frequency. (The numbers along the ordinate should be divided by $\sqrt{2}$.) The phonon notation is the same as in Fig. 6. In the case of Si and Ge the curves are almost identical, so that the curves for Si are shown only where they deviate significantly from the corresponding curves for Ge.

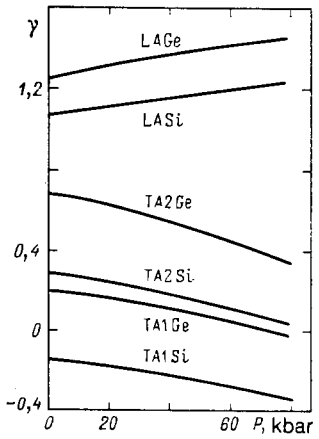

FIG. 9. Pressure dependences of the Grüneisen mode parameters of long-wavelength acoustic modes of Si and Ge (Ref. 84). Here, TA1 and TA2 are transverse acoustic modes associated with the elastic moduli $(C_{11} - C_{12})/2$ and C_{44}, respectively; LA is a longitudinal acoustic mode related to the elastic modulus C_{11}.

zone. High-pressure Raman scattering measurements indicate that at the edge of the Brillouin zone (at the points X, L, etc.) these modes can have negative Grüneisen parameters,[13,82,83] which are usually attributed to the instability of the crystal lattice. Therefore, an empirical linear relationship (Fig. 8) has been proposed[82] between the pressure of the transition to the metallic state and the Grüneisen parameter of the TA(X) mode.

In the limit of long wavelengths the slopes of the dispersion curves of acoustic phonons govern the velocities of propagation of sound in a crystal. Measurements of the travel times of ultrasonic waves in Si and Ge at various hydrostatic pressures[84] demonstrated a reduction in the velocity of transverse acoustic waves related to the elastic force constants $(C_{11} - C_{12})/2$ and C_{44} on approach to the $\alpha \rightarrow \beta$ transition point. The velocities of longitudinal waves were found to increase. Figure 9 gives the pressure dependences of the microscopic Grüneisen parameters of the corresponding modes illustrating this behavior. It is worth noting the specific behavior of the Grüneisen parameters of the TA1 modes of Si and Ge indicating a reduction in the rigidity of the crystal lattices of these elements on approach to the phase transition point.

A comparison of the data on the phonon modes of Si, Ge, and C (Fig. 7) shows that carbon does not fit the general rules (properties of the binary compounds with the zinc-blende structure are similar to the data on Si and Ge). Diamond does not exhibit a characteristic flattening of the TA branches far from the center of the Brillouin zone; the frequencies of the corresponding phonons (normalized to the plasma frequency) are considerably higher. The slope of the initial parts of the TA branches near the point Γ (in relative units) is also much greater for diamond. Moreover, there are several differences in the case of the high-lying phonon branches (Fig. 7). First of all, it is worth noting a different sequence of the phonon branches at the points X and L (in

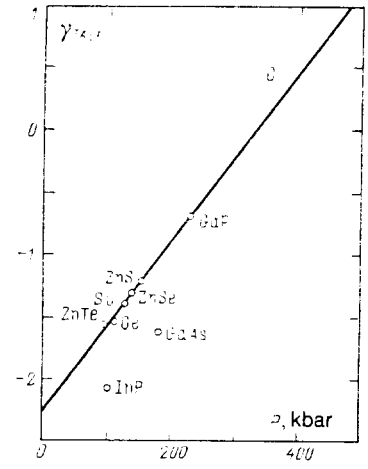

FIG. 8. Relationship between the Grüneisen parameters of the TA(X) modes and the pressures of the transition to a metallic phase in various tetrahedral compounds.[82,83] In the case of diamond we have $\gamma_{TA(X)} = 0.4 \pm 0.9$ (Ref. 89).

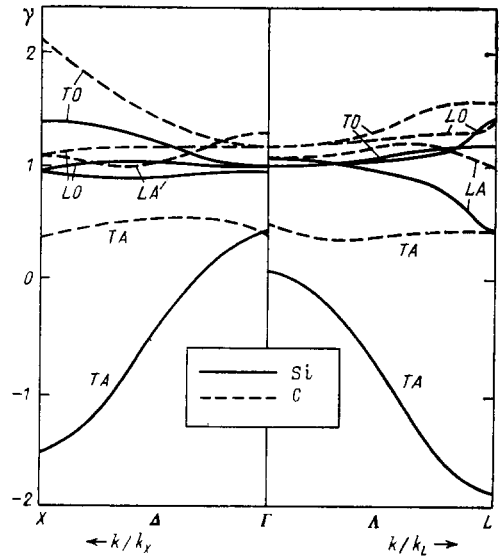

FIG. 10. Grüneisen parameters of diamond[89] and silicon[90] calculated for the [100] (Δ) and [111] (Λ) directions.

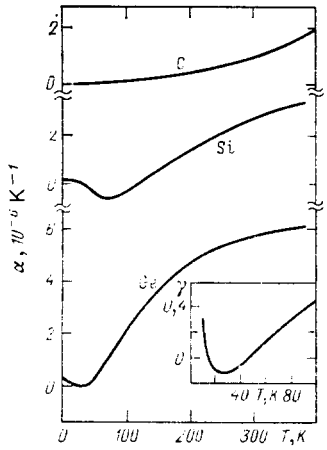

FIG. 11. Temperature dependences of the linear expansion coefficients of C (diamond), Si, and Ge (Ref. 91). The inset shows the temperature dependence of the Grüneisen parameter γ of germanium.

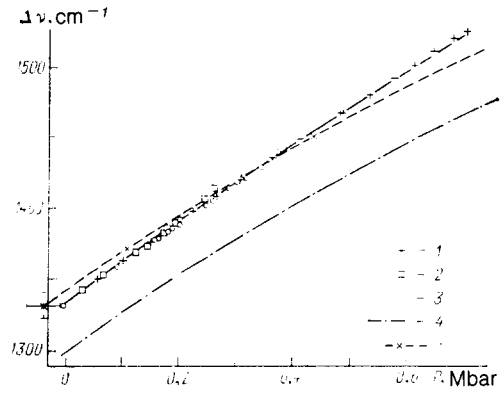

FIG. 12. Pressure dependences of the frequency of the maximum of a first-order Raman band. Results of experimental investigations: 1) Ref. 64; 2) Ref. 65; 3) Ref. 66. Theoretical calculations: 4) Ref. 80; 5) Ref. 66.

diamond the LO mode is higher than the TO mode, whereas the reverse is true of Si and Ge). Moreover, it has been shown[78,85–87] that the absolute maximum of the dispersion branches of diamond is located along the [100] direction in the case when $k \approx (1/3)k_X$ (k_X is the wave vector at the point X at the edge of the Brillouin zone), whereas in the case of Si and Ge the absolute maximum is at the point Γ. All these features indicate that the noncentral interactions (mentioned above) play a much greater role in diamond than they do in Si and Ge. Therefore, diamond behaves in a special manner also under the action of external forces. Determination of the elastic properties[88] and of the Raman spectra under pressure[89] has demonstrated that the Grüneisen parameters of diamond are positive for all the phonon branches (Fig. 10) and, consequently, the linear expansion coefficient is positive throughout the investigated range of temperatures (Fig. 11).

For the sake of comparison, Figs. 10 and 11 give also the data for Si and Ge which demonstrate typical behavior of tetrahedral semiconductors with negative Grüneisen parameters of the transverse acoustic modes and negative linear expansion coefficients at low temperatures. It should be stressed that the positive Grüneisen parameters of all the phonon modes of diamond are evidence of the stability of its lattice at moderate pressures. However, and investigation of the stability of diamond at ultrahigh pressures should include a study of the changes in the Grüneisen parameters (see, for example, Fig. 9) at higher pressures. Quite recently[64] it had become possible to investigate the behavior of the Grüneisen parameter of an optical mode at the center of the Brillouin zone. This was done by investigating first-order Raman spectra of diamond (see also Refs. 65 and 66). Experiments were carried out in a cell with diamond anvils and samples of diamond were under quasihydrostatic conditions surrounded by compressed xenon. Figure 12 shows the results of a determination of the spectral position of the maximum of the first-order band of diamond as a function of the applied pressure. This figure includes, for the sake of comparison, the experimental results from Refs. 65 and 66 and also fragments of theoretical curves calculated for the range 0–600 GPa (Refs. 66 and 80).

We shall now compare the experimental data on the first-order Raman scattering in C (diamond), Si, and Ge (Refs. 13 and 83). In view of the smallness of the relative value of the frequency shift $\Delta\nu/\nu_0$ in the investigated range of pressures, the dependence $P(\nu)$ can be represented by an expansion

$$\frac{P}{K_0} = A_1 \frac{\Delta\nu}{\nu_0} + A_2 \left(\frac{\Delta\nu}{\nu_0}\right)^2, \qquad (1)$$

where P is the applied pressure; K_0 is the bulk modulus at $P = 0$; ν and ν_0 are the actual and initial values of the optical phonon frequencies; $\Delta\nu = \nu - \nu_0$. The experimental data[64,13,83] can be approximated by Eq. (1) using the following values of the coefficients:

$$\begin{array}{lll} \text{C:} & A_1 = 1.000 \pm 0.003, & A_2 = 1.02 \pm 0.05, \\ \text{Si:} & A_1 = 1.00 \pm 0.03, & A_2 = 2.31 \pm 0.33, \\ \text{Ge:} & A_1 = 0.95 \pm 0.03, & A_2 = 2.09 \pm 0.33. \end{array} \qquad (2)$$

The values of A_1 found in this way [it should be pointed out that $A_1 = (\nu_0/K_0)(\partial P/\partial\nu)_{\nu_0} = 1/\gamma_0$] can be used to calculate directly the mode Grüneisen parameters, the values of which are listed in Table I. In the case of diamond the value

TABLE I. Bulk moduli, Grüneisen mode parameters, and their derivatives with respect to pressure for C (diamond), Si, and Ge.

	P_c	K_0	$(\partial K/\partial P)_0$	γ_0	$(\partial\gamma/\partial P)_0$
C	>2750 [a]	4420 [d]	4±0.7 [d]	1.000±0.003 [f]	2.2±1.6 [f]
Si	125 [b]	970.8 [e]	4.16 [e]	1.00±0.03 *	−1.5±0.6 *
Ge	110 [c]	724.3 [e]	4.35 [e]	1.05±0.03 *	−1.9±1.0 *

Here, P_c is the critical pressure of the transition to the β-Sn structure (kbar); K_0 is in kilobars; $(\partial\gamma/\partial P)_0$ is in units of 10^{-4} kbar^{-1}; the values identified by a–f are taken from Refs. 62, 13, 83, 88, 94, and 64, respectively; *calculated from the experimental data of Refs. 13 and 83, represented in the form given by Eq. (1).

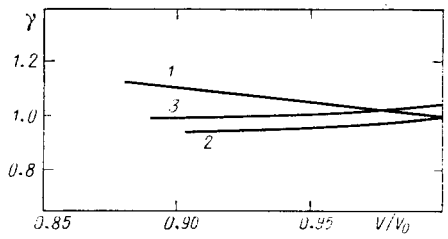

FIG. 13. Volume dependences of Grüneisen parameters of the LTO(Γ) modes of diamond, Si, and Ge (Ref. 64). The values of γ are calculated using the Murnaghan equation. The data used in the calculations are listed in Table I. Designation of the curves: 1) diamond; 2) Si; 3) Ge.

$\gamma_0 = 1 \pm 0.003$ is in excellent agreement with the results reported in Refs. 65, 66, 92, and 93. In the case of Si and Ge the values reported in Ref. 64 differ somewhat from those given in the original papers[13,83] and this is probably due to the different nature of the approximating functions used in Ref. 64, on the one hand, and in Refs. 13 and 83, on the other.

The coefficient A_2 in Eq. (1) can be used to find the initial derivative of the Grüneisen parameter with respect to the applied pressure $(\partial\gamma/\partial P)_0$. In fact, since

$$A_2 = \frac{v_0^2}{2K_0}\left(\frac{\partial^2 P}{\partial v^2}\right)_{v_0} = \frac{1}{2}\left[\left(\frac{\partial K}{\partial P}\right)A_1^2 - K_0\left(\frac{\partial\gamma}{\partial P}\right)_0 A_1^3 - A_1\right], \quad (3)$$

we find that $(\partial\gamma/\partial P)_0 = (1/K_0)[(\partial K/\partial P)_0\gamma_0 - \gamma_0^2 - 2A_2\gamma_0^3]$.

Substituting the known values of $(\partial K/\partial P)_0$ and K_0 in Eq. (3), we find that the initial slope of the dependence $\gamma(P)$ is positive for diamond (see also Ref. 100), in contrast to Si and Ge for which this slope is negative (Table I). This difference between the nature of these dependences is retained also at high pressures (Fig. 13).

It should be pointed out that the similarity of the values of $(\partial K/\partial P)_0$ for diamond, Si, and Ge (Table I) is evidence of the existence of a universal equation of state for these substances at moderate pressures. Therefore, the differences between the nature of changes in the parameter γ of diamond, Si, and Ge are clearly a consequence of the different volume dependences of the noncentral interactions stabilizing their tetrahedral structures,[74] but making no significant contribution to the bulk compressibility. The increase in the parameter γ of diamond with increase in pressure thus means that the applied pressure stabilizes the tetrahedral structure of diamond, in contrast to Si and Ge, which undergo the $\alpha \rightarrow \beta$ transition at relatively low pressures.

Anticipating somewhat the discussion in the next section, we note that the reason for the unique stability of the diamond phase of carbon should be related to the characteristics of its electron structure.[1] The absence of the p electrons from the ionic core of carbon results in a considerable reduction in the energy of the sp^3 hybrid states in carbon (see next section), which is responsible for the unique stability of the loosely packed diamond structure, and also for the enormous relative increase of the range of existence of the diamond structure in the P-T diagram, compared with structural analogs of diamond. If this approach is valid, then another such stable substance should be the closest electronic analog of diamond which is boron nitride in its cubic modification (Borazon). A preliminary determination of first-order Raman spectra of Borazon, carried out in our laboratory, supported this point of view. It should be pointed out that more reliable conclusions could be drawn on the basis of second-order Raman spectra of diamond and Borazon at ultrahigh pressures, because in this case it should be possible to study the behavior of the mode Grüneisen parameters of transverse acoustic modes.

4. "WHAT WILL HAPPEN TO DIAMOND AT MEGABAR PRESSURES?"

The progress in generation of ultrahigh static pressures by the diamond anvil method[61] has stimulated new theoretical treatments of the problem of the stability of diamond. Yin and Cohen[1] calculated the total energies of the diamond phase of carbon, and also of five metallic phases with the following structures: white tin (β), simple cubic (sc), face-centered cubic (fcc), body-centered cubic (bcc), and hexagonal close-packed (hcp). In these calculations they used the pseudopotential method within the framework of the formalism of the local density function. This method was found to be extremely fruitful in the prediction of the parameters of phase transitions in Si and Ge (Refs. 95–97). Figure 14a shows the calculated dependences of the total energy of the predicted carbon phases as a function of the volume. We can see from this figure that diamond is stable against transitions to the five metallic phases listed above in the range of relative compressions from 1 to 0.6, corresponding to pressures up to ~5 Mbar. It should be noted that a similar calculation carried out for Si (Fig. 14b) is in excellent agreement with the

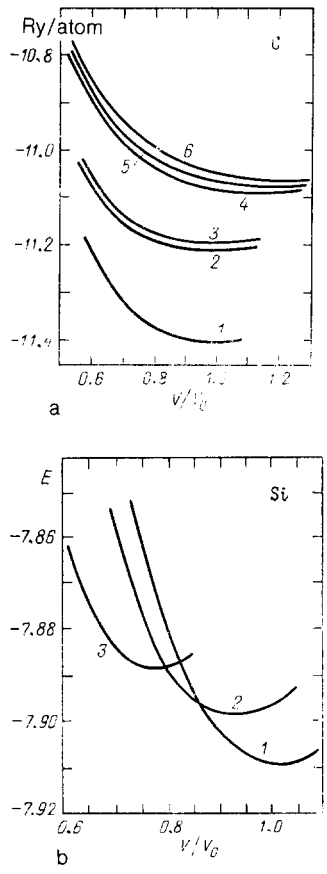

FIG. 14. Total energy plotted as a function of the volumes of high-pressure phases of carbon (a) and silicon (b) on the basis of Refs. 1 and 95, respectively. *a*: 1) α; 2) sc; 3) β; 4) bcc; 5) hcp; 6) fcc. *b*: 1) α; 2) BC-8; 3) β.

TABLE II. Transition pressures and volumes calculated for three phase transitions of carbon between α, sc, and BC-8 modifications[98] (volumes are normalized to the equilibrium volume of the structure of diamond under normal conditions).

	Transition pressure, Mbar	Initial volume	Final volume
$\alpha \rightarrow$ BC-8	12	0.468	0.456
BC-8 $\rightarrow$ sc	27	0.345	0.326
$\alpha \rightarrow$ sc	22	0.379	0.352

experimental data[10,15-17] on the pressure needed for the $\alpha \rightarrow \beta$ transition and on the volumes of the corresponding phases at the transition point. The equilibrium volumes of the metallic phases of carbon are very large (Fig. 14a), in contrast to the metallic states of Si and Ge which are approximately 20% denser than the α phase. This is the reason why it is very difficult to metallize diamond. Among the metallic phases of carbon mentioned above the one which is most favorable from the energy point of view is the sc structure (and not β, as in the case of Si and Ge): calculations indicate that the transition to this structure should occur at a pressure of $\sim$23 Mbar and it should be accompanied by a reduction in the volume by $\sim$6% (Table II). Therefore, a more detailed theoretical calculation destroys the scaling hypothesis (see Sec. 1). Physical interpretation of the special properties of diamond given in Ref. 1 is based on the electronic configuration of carbon. Since in contrast to Si and Ge, the ionic core of carbon does not contain p electrons, it follows that the valence p electrons of carbon are located much closer to the nucleus (compared with the s electrons) than in the case of Si and Ge. This effect plays an important role in the formation of the structure of diamond, because in the case of sp^3 hybridization the role of the p electron states becomes more important. Moreover, since the lowest vacant carbon orbitals (d) have the quantum number $n + 1$ (ns and np are the filled valence orbitals), compared with n for Si and Ge, the dimensions of these orbitals are considerably greater than those of the corresponding orbitals of Si and Ge. Since the chemical binding in metallic phases is influenced considerably by the vacant d states, this explains why the equilibrium volumes of the metallic phases of carbon are so large. Since this conclusion is based on general considerations, which apply equally well to various metallic phases, we can expect the transformation of diamond to another (not mentioned above) metallic phase to occur also at very high pressures (> 10 Mbar).

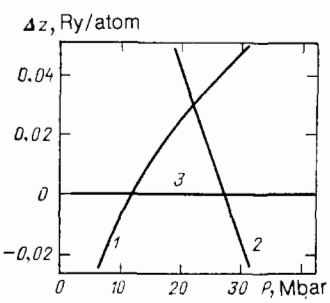

FIG. 15. Pressure dependences of the Gibbs thermodynamic potential (in relative units) taken from Ref. 98: 1) α; 2) BC-8; 3) sc. The horizontal axis represents the thermodynamic potential of the BC-8 phase and should be regarded as the reference level.

Developing further the ideas of Yin and Cohen,[1] we can postulate that compression of the diamond phases of Si and Ge should increase the density of the p electrons in the ionic core and this should favor dehybridization of the covalent bonds and make the tetrahedral phases unstable. On the other hand, compression of diamond should favor an increase in the rigidity of the tetrahedral structure, because it increases the overlap of the sp^3-hybridized orbitals.

It is therefore clear that the diamond phase of carbon is effectively more compact than any other possible metallic structures with much higher (compared with diamond) coordination numbers. Hence, it follows in particular that the α phase of carbon can be even denser than the metallic liquid at the same temperature, i.e., the melting curve of diamond may differ from Si and Ge in respect of its positive slope (see Sec. 1).

It was proposed in Refs. 98 and 99 that carbon has a high-pressure phase isostructural with the known metastable phase of silicon which has the BC-8 structure (see Fig. 3). The structure of this phase consists of weakly distorted tetrahedra without a significant change in the coordination of the atoms or in the nature of the interaction between them, compared with the diamond lattice. Since we have seen that in the case of carbon the formation of chemical bonds directly by the sp^3-hybridized orbitals is very favorable from the energy point of view, we can conclude that the BC-8 structure is in fact the most probable candidate for the phase of diamond at high pressures. Calculations similar to those mentioned above have indicated that, in contrast to Si for which the BC-8 phase is metastable, diamond may go over to this phase at pressures which are even lower than that at which the $\alpha \rightarrow \beta$ transformation takes place (see Table II). Figure 15 shows the Gibbs thermodynamic potentials (in relative units) of the α, BC-8, and sc phases of carbon as a function of pressure. We can see from Fig. 14 that diamond initially goes over to the BC-8 phase and then to the sc phase. However, since the activation energy of the $\alpha \rightarrow$ BC-8 transition is high, the possibility of the direct $\alpha \rightarrow$ sc transition was not excluded in Refs. 98 and 99. Nevertheless, above 12 Mbar the BC-8 phase is preferred for thermodynamic reasons and this pressure represents a new limit to the stability of diamond.

We shall conclude by noting that at high pressures we can expect diamond to transform generally into some other metallic semiconducting phase with a structure about which we know nothing at present. This possibility is of considerable interest and it should be investigated in the future.

The author is grateful to S. M. Stishov for stimulating discussions and his interest, and to I. N. Makarenko for valuable comments.

[1)]The packing fraction of the diamond structure represented by a system of spheres is 34%, whereas the packing fraction of the same system of spheres arranged to ensure the closest packing is 74%.

[2)]It should be noted that 1 bar $= 10^5$ N/m$^2 \approx 0.987$ atm ≈ 1.020 kgf/cm^2.

[3)]In the case of tin this part of the phase diagram is located at "negative" pressures.

[4)]In the case of Si and Ge the γ phase is located at "negative" pressures.[3,31]

[5)]The work of Jamieson[10,53] established that "phase III" has the tetragonal lattice of the β-Sn type.

[1]M. T. Yin and M. L. Cohen, Phys. Rev. Lett. **50**, 2006 (1983).
[2]A. Jayaraman, W. Klement Jr., and G. C. Kennedy, Phys. Rev. **130**, 540 (1963).
[3]F. P. Bundy, J. Chem. Phys. **41**, 3809 (1964).
[4]J. Lees and B. H. J. Williamson, Nature (London) **208**, 278 (1965).
[5]S. E. Babb Jr., J. Chem. Phys. **37**, 922 (1962).
[6]G. C. Kennedy and R. C. Newton, in: *Solids Under Pressure* (ed. by W. Paul and D. M. Warschauer), McGraw-Hill, New York (1963), p. 163.
[7]D. L. Decker, J. D. Jorgensen, and R. W. Young, High Temp. High Press. 7, 331 (1975).
[8]S. N. Vaidya, J. Akella, and G. C. Kennedy, J. Phys. Chem. Solids **30**, 1411 (1969).
[9]S. Minomura and H. G. Drickamer, J. Phys. Chem. Solids **23**, 451 (1962).
[10]J. C. Jamieson, Science **139**, 762 (1963).
[11]F. P. Bundy and J. S. Kasper, Science **139**, 340 (1963).
[12]J. F. Cannon, J. Phys. Chem. Ref. Data **3**, 781 (1974).
[13]B. A. Weinstein and G. J. Piermarini, Phys. Rev. B **12**, 1172 (1975).
[14]G. J. Piermarini and S. Block, Rev. Sci. Instrum. **46**, 973 (1975).
[15]Z. V. Malyushitskaya and S. S. Kabalkina, Fiz. Tverd. Tela (Leningrad) **26**, 2259 (1984) [Sov. Phys. Solid State **26**, 1370 (1984)].
[16]H. Olijnyk, S. K. Sikka, and W. B. Holzapfel, Phys. Lett. A **103**, 137 (1984); H. Olijnyk and W. B. Holzapfel, J. Phys. (Paris) **45**, Colloq. 8, C8-153 (1984).
[17]J. Z. Hu and I. L. Spain, Solid State Commun. **51**, 263 (1984); I. L. Spain, J. Z. Hu, C. S. Menoni, and D. Black, J. Phys. (Paris) **45**, Colloq. 8, C8-407 (1984).
[18]A. Werner, J. A. Sanjurjo, and M. Cardona, Solid State Commun. **44**, 155 (1982).
[19]M. Baublitz Jr. and A. L. Ruoff, J. Appl. Phys. **53**, 5669 (1982).
[20]S. B. Qadri, E. F. Skelton, and A. W. Webb, J. Appl. Phys. **54**, 3609 (1983).
[21]M. N. Pavlovskiĭ, Fiz. Tverd. Tela (Leningrad) **9**, 3192 (1967) [Sov. Phys. Solid State **9**, 2514 (1968)].
[22]H. Enz, Diploma Thesis, Eidgenossische technische Hochschul, Zürich (1951).
[23]I. N. Nikolaev, V. P. Mar'in, V. N. Panyushkin, and L. S. Pavlyukov, Fiz. Tverd. Tela (Leningrad) **14**, 2337 (1972) [Sov. Phys. Solid State **14**, 2022 (1973)].
[24]R. H. Wentorf Jr. and J. S. Kasper, Science **139**, 338 (1963).
[25]J. S. Kasper and S. M. Richards, Acta Crystallogr. **17**, 752 (1964).
[26]C. H. Bates, F. Dachille, and R. Roy, Science **147**, 860 (1965).
[27]A. Grüttner, R. Nesper, and H. G. von Schnering, Angew. Chem. **94**, 933 (1982) [Angew. Chem. Intern. Ed. Eng. **21**, 912 (1982)].
[28]D. J. Chadi, Phys. Rev. B **32**, 6485 (1985).
[29]F. P. Bundy, J. Geophys. Res. **85**, 6930 (1980); Solid State Physics Under Pressure, Recent Advances with Anvil Devices (Proc. Intern. Conf., Izu-Nagaoka, Japan, 1984, ed. by S. Minomura), publ. by Reidel, Dordrecht, Netherlands (1985), p. 1.
[30]R. Clarke and C. Uher, Adv. Phys. **33**, 469 (1984).
[31]M. T. Yin and M. L. Cohen, Phys. Rev. B **29**, 6996 (1984).
[32]F. P. Bundy, H. P. Bovenkerk, H. M. Strong, and R. H. Wentorf Jr., J. Chem. Phys. **35**, 383 (1961).
[33]C. S. Kennedy and G. C. Kennedy, J. Geophys. Res. **81**, 2467 (1976).
[34]F. D. Rossini and R. S. Jessup, J. Res. Natl. Bur. Stand. **21**, 491 (1938).
[35]O. I. Leĭpunskiĭ, Usp. Khim. **8**, 1519 (1939).
[36]R. Berman and F. Simon, Z. Elektrochem. **59**, 335 (1955).
[37]F. P. Bundy, Science **137**, 1055 (1962); J. Chem. Phys. **38**, 618 (1963).
[38]N. S. Fateeva and L. F. Vereshchagin, Pis'ma Zh. Eksp. Teor. Fiz. **13**, 157 (1971) [JETP Lett. **13**, 110 (1971)]; L. F. Vereshchagin and N. S. Fateeva, Zh. Eksp. Teor. Fiz. **55**, 1145 (1968) [Sov. Phys. JETP **28**, 597 (1969)].
[39]F. P. Bundy, a) Science **137**, 1057 (1962); b) J. Chem. Phys. **38**, 631 (1963).
[40]R. B. Aust and H. G. Drickamer, Science **140**, 817 (1963).
[41]F. P. Bundy and J. S. Kasper, J. Chem. Phys. **46**, 3437 (1967).
[42]F. R. Corrigan and F. P. Bundy, J. Chem. Phys. **63**, 3812 (1975).
[43]R. E. Hanneman, H. M. Strong, and F. P. Bundy, Science **155**, 995 (1967).
[44]B. J. Alder and R. H. Christian, Phys. Rev. Lett. **7**, 367 (1961).
[45]P. S. DeCarli and J. C. Jamieson, Science **133**, 1821 (1961).
[46]M. N. Pavlovskiĭ and V. P. Drakin, Pis'ma Zh. Eksp. Teor. Fiz. **4**, 169 (1966) [JETP Lett. **4**, 116 (1966)].
[47]R. F. Trunin, G. V. Simakov, B. N. Moiseev, L. V. Popov, and M. A. Podurets, Zh. Eksp. Teor. Fiz. **56**, 1169 (1969) [Sov. Phys. JETP **29**, 628 (1969)].
[48]W. H. Gust, Phys. Rev. B **22**, 4744 (1980).
[49]V. I. Trefilov, G. I. Savvakin, V. V. Skorokhod, Yu. M. Solonin, and A. F. Khrienko, Dokl. Akad. Nauk SSSR **239**, 838 (1978) [Sov. Phys. Dokl. **23**, 269 (1978)].
[50]Netherlands Patent No. 6 506 395, publ. November 22 (1965).
[51]L. F. Trueb, J. Appl. Phys. **39**, 4707 (1968); **42**, 503 (1971).
[52]J. W. Shaner, J. M. Brown, C. A. Swenson, and R. G. McQueen, J. Phys. (Paris) **45**, Colloq. 8, C8-235 (1984).
[53]J. C. Jamieson, Science **139**, 845 (1963).
[54]M. J. P. Musgrave, Proc. Phys. Soc. London **84**, 585 (1964).
[55]C. Weigel, R. P. Messmer, and J. W. Corbett, Solid State Commun. **13**, 723 (1973).
[56]L. F. Vereshchagin, E. N. Yakovlev, G. N. Stepanov, and B. V. Vinogradov, Pis'ma Zh. Eksp. Teor. Fiz. **16**, 382 (1972) [JETP Lett. **16**, 270 (1972)].
[57]L. F. Vereshchagin, E. N. Yakovlev, B. V. Vinogradov, V. P. Sakun, and G. N. Stepanov, High Temp. High Press. **6**, 505 (1974).
[58]J. A. Van Vechten, Phys. Rev. B **7**, 1479 (1973).
[59]R. Grover, in: High Pressure Science and Technology (Proc. Seventh Intern. AIRAPT Conf., Le Creusot, France, 1979, ed. by B. Vodar and Ph. Marteau), Vol. 1, Pergamon Press, Oxford (1980), p. 251.
[60]M. N. Pavlovskiĭ, Fiz. Tverd. Tela (Leningrad) **13**, 893 (1971) [Sov. Phys. Solid State **13**, 741 (1971)].
[61]H. K. Mao and P. M. Bell, Science **200**, 1145 (1978).
[62]P. M. Bell, H. K. Mao, and K. Goettel, Science **226**, 542 (1984); K. A. Goettel, H. K. Mao, and P. M. Bell, Rev. Sci. Instrum. **56**, 1420 (1985).
[63]J. A. Xu, H. K. Mao, and P. M. Bell, Paper presented at Tenth Intern. Conf. on High Pressure Science and Technology, Amsterdam, 1985.
[64]A. F. Goncharov, I. N. Makarenko, and S. M. Stishov, Pis'ma Zh. Eksp. Teor. Fiz. **41**, 150 (1985) [JETP Lett. **41**, 184 (1985)].
[65]H. Boppart, J. van Straaten, and I. F. Silvera, Phys. Rev. B **32**, 1423 (1985).
[66]M. Hanfland, K. Syassen, S. Fahy, S. G. Louie, and M. L. Cohen, Phys. Rev. B **31**, 6896 (1985).
[67]M. Hanfland and K. Syassen, J. Appl. Phys. **57**, 2752 (1985).
[68]P. N. Keating, Phys. Rev. **145**, 637 (1966).
[69]R. M. Martin, Phys. Rev. **186**, 871 (1969); Phys. Rev. B **1**, 4005 (1970).
[70]W. Weber, Phys. Rev. B **15**, 4789 (1977).
[71]R. Tubino, L. Piseri, and G. Zerbi, J. Chem. Phys. **56**, 1022 (1972).
[72]S. K. Sinha, CRC Crit. Rev. Solid State Sci. **3**, 273 (1973).
[73]E. O. Kane, Phys. Rev. B **31**, 7865 (1985).
[74]M. T. Yin and M. L. Cohen, Phys. Rev. B **26**, 3259 (1982).
[75]M. T. Yin and M. L. Cohen, Phys. Rev. B **25**, 4317 (1982).
[76]B. N. Harmon, W. Weber, and D. R. Hamann, Phys. Rev. B **25**, 1109 (1982).
[77]H. Wendel and R. M. Martin, Phys. Rev. B **19**, 5251 (1979).
[78]D. Vanderbilt, S. G. Louie, and M. L. Cohen, Phys. Rev. Lett. **53**, 1477 (1984).
[79]O. H. Nielsen and R. M. Martin, Phys. Rev. B **32**, 3792 (1985).
[80]O. H. Nielsen, Preprint No. NORDITA-85/40, Copenhagen (1985); Phys. Rev. B (in press).
[81]M J. P. Musgrave, Proc. R. Soc. London Ser. A **272**, 503 (1963).
[82]B. A. Weinstein, Solid State Commun. **24**, 595 (1977).
[83]D. Olego and M. Cardona, Phys. Rev. B **25**, 1151 (1982).
[84]V. A. Goncharova, E. V. Chernysheva, and F. F. Voronov, Fiz. Tverd. Tela (Leningrad) **25**, 3680 (1983) [Sov. Phys. Solid State **25**, 2118 (1983)].
[85]R. Tubino and J. L. Birman, Phys. Rev. Lett. **35**, 670 (1975); Phys. Rev. B **15**, 5843 (1977).
[86]S. Go, H. Bilz, and M. Cardona, Phys. Rev. Lett. **34**, 580 (1975).
[87]K. Uchinokura, T. Sekine, and E. Matsuura, J. Phys. Chem. Solids **35**, 171 (1974).
[88]H. J. McSkimin and P. Andreatch Jr., J. Appl. Phys. **43**, 3944 (1972).
[89]B. J. Parsons, Proc. R. Soc. London Ser. A **352**, 397 (1976).
[90]A. P. Mayer and R. K. Wehner, Phys. Status Solidi B **126**, 91 (1984).
[91]G. Dolling and R. A. Cowley, Proc. Phys. Soc. London **88**, 463 (1966).
[92]S. S. Mitra, O. Brafman, W. B. Daniels, and R. K. Crawford, Phys. Rev. **186**, 942 (1969).

[93]E. Whalley, A. Lavergne, and P. T. T. Wong, Rev. Sci. Instrum. **47**, 845 (1976).
[94]O. L. Anderson, J. Phys. Chem. Solids **27**, 547 (1966).
[95]M. T. Yin and M. L. Cohen, Phys. Rev. B **26**, 5668 (1982).
[96]K. J. Chang and M. L. Cohen, Phys. Rev. B **30**, 5376 (1984); **31**, 7819 (1985).
[97]R. J. Needs and R. M. Martin, Phys. Rev. B **30**, 5390 (1984).
[98]M. T. Yin, Phys. Rev. B **30**, 1773 (1984).
[99]R. Biswas, R. M. Martin, R. J. Needs, and O. H. Nielsen, Phys. Rev. B **30**, 3210 (1984).
[100]I. V. Aleksandrov, A. F. Goncharov, and S. M. Stishov, Pis'ma Zh. Eksp. Teor. Fiz. **44**, 474 (1986) [JETP Lett. **44**, 611 (1986)].

Translated by A. Tybulewicz